www.czasopisma.pan.pl PAN POLSKA AKADEMIA NAUK www.journals.pan.pl

DE GRUYTER OPEN GOSPODARKA SUROWCAMI MINERALNYMI – MINERAL RESOURCES MANAGEMENT
2017 Volume 33 Issue 1 Pages 93–110
DOI 10.1515/gospo-2017-0010

EWA LEWICKA*

Phase transitions of ferruginous minerals in the course of thermal processing of feldspar-quartz raw materials from the Sobótka region (Lower Silesia)

Introduction

This paper presents the results of phase and chemical investigations of feldspar-quartz raw materials from deposits of leucogranites located in the Sobótka region and constitutes a continuation of research conducted by the author in 2011–2015 aimed at establishing forms and concentrations of colouring compounds and elements as well reasons for colour variation of the examined samples after firing (Lewicka 2013, 2015, 2016a, 2016b; Lewicka and Franus 2014). These studies revealed the presence of minerals enriched in colouring components, e.g. transition elements such as: Fe, Ti, Mn, Ni and Cu, as well as some REE (Ce, Nd) and actinides (Th, U). From the above-mentioned transition elements the dominant colour contributor is iron, the most plentiful in nature. Its main mineral phases ascertained in the examined samples in the course of previous optical and scanning electron microscopy observations coupled with local EDS measurements are as follows: chlorites, biotite – chloritized to a various degree, light micas (muscovite, sericite), rutile, Fe,Mn-rich garnets, as well as – although to a limited extent – also kaolinite, feldspars, monazite, sphalerite, xenotime, zircon, and epidote (Fe-rich pistacite). Occasionally, also some small quantities of iron

* Ph.D. Eng., The Mineral and Energy Economy Research Institute of the Polish Academy of Sciences, Krakow, Poland; e-mail: lewicka@min-pan.krakow.pl

www.czasopisma.pan.pl PAN POLSKA AKADEMIA NAUK www.journals.pan.pl

own minerals were observed, i.e. pyrite and titanomagnetite or magnetite. Other colouring elements detected in the samples in the course of EDS chemical analyses were the following: Mn (in chlorites, biotite, and garnets), Th, U, Ce, Nd (mainly in monazite), Ti, V (in rutile), U (in zircon), and REE (in xenotime).

The research presented in the paper covered the firing of the samples of various contents of colouring components in two cycles: the standard one, lasting more than 2 hours, and the fast one, performed in conditions analogous to the current technology of ceramic tile manufacturing, the duration of which does not exceed 1 hour. The obtained bodies were examined by X-ray powder diffraction (XRD), scanning microscopy SEM-EDS, and Mössbauer spectroscopy methods. The main purpose of these investigations was to determine the phase evolution that developed during thermal treatment of the samples, with a special focus on ferruginous minerals.

1. Materials and methods

The subject of the research were samples of feldspar-quartz raw materials from deposits operated by the Strzeblowskie Mineral Mines (SKSM) in the Sobótka region, i.e.: Pagórki Zachodnie (PZ), Stary Łom (SL) and Strzeblów I (SI). The samples were prepared from averaged drill cuttings from exploratory boreholes made on these deposits between December 2015 and August 2016. The chemical composition of the samples was determined by the wet method on the Nanocolor UV/VIS spectrometer and BW flame photometer (Table 1). The research was conducted on the material characterized by the highest content of colouring oxides (mainly Fe_2O_3) and optically the darkest colour. Two pellets were formed from each of the samples, which were fired in different conditions: one in the standard cycle and the other – in the fast one. The standard cycle was performed in the L08/14 Nabertherm laboratory furnace, in which the firing regime was as follows: maximum temperature 1200°C reached in 2 hours, soaking time – 15 minutes, cooling – gradual, to room temperature, inside the furnace chamber. Firing in the fast cycle, in conditions similar to those commonly employed in the contemporary ceramic tile industry, was carried out in the LS 25/13 Nabertherm laboratory furnace, in which the maximum temperature 1260°C was reached in 22 minutes; the sample was cooled (quenched) outside the furnace for 22 minutes after soaking time that lasted 7 minutes. The purpose of running these two parallel experiments was to find – in course of further examinations – the differences in phase composition and microstructure of the bodies obtained in short and long-lasting thermal treatment, respectively. After firing, the colour parameters of all the samples (expressed as L*, a* and b* chromatic coordinates) were measured by a UV-Vis Minolta CM-2300D spectrophotometer.

Three pairs of pellets fired in two different cycles were examined by a scanning electron microscope, while one of them, characterized by the highest contents of iron oxide (SI-1j and SI-1c), underwent Mössbauer spectroscopy measurements. The phase composition of

Table 1. Chemical composition of drill cuttings from exploratory boreholes in the Strzeblow I (SI-1), Stary Lom (SL-2), and Pagorki Zachodnie (PZ) deposits, and colour parameters of pellets made thereof after thermal treatment in standard (j) and fast (c) firing cycles

Tabela 1. Skład chemiczny próbek zwiercin z rozpoznawczych otworów wiertniczych ze złóż: Strzeblów I (SI-1), Stary Łom (SL-2) i Pagórki Zachodnie (PZ-3), oraz parametry barwy wykonanych z nich pastylek poddanych obróbce termicznej w standardowym (j) i szybkim (c) cyklu wypalania

Sample	SiO_2 [%]	Al_2O_3 [%]	Na_2O [%]	K_2O [%]	Fe_2O_3 [%]	TiO_2 [%]	Colour parameters after firing in the standard cycle (j)			Colour parameters after firing in the short cycle (c)		
							L* [%]	a*	b*	L* [%]	a*	b*
SI-1	75.2	14.7	3.92	3.51	1.70	0.24	47.3	1.59	5.40	41.1	3.96	3.23
SL-2	75.5	13.7	4.53	4.21	1.28	0.07	46.7	5.24	5.14	44.2	9.18	7.20
PZ-3	76.7	13.2	4.41	4.27	0.67	–	51.3	4.42	4.77	45.6	9.68	7.26

another pair of the fired bodies (PZ-3j and PZ-c) was determined by X-ray powder diffraction (XRD) on a diffractometer equipped with a lamp with a Cu anode for the line Kα. Microstructural features of the samples were observed on their fracture surfaces after sputtering with a thin layer of carbon, using a HITACHI S-4700 scanning electron microscope. Qualitative EDS (NORAN Vantage system) chemical analyses were made simultaneously with SEM observations. In order to detect concentrations of iron and other colouring elements (including REE) the research was carried out in back-scattered electron mode (BSE). Mössbauer spectroscopy measurements were performed in the transmission mode using a RENON MsAa-3 spectrometer equipped with a LND Kr-filled proportional detector and a He-Ne laser based interferometer used to calibrate velocity scale (Górnicki et al. 2007). A single line commercial ^{57}Co (Rh) source kept at room temperature was applied for 14.41-keV resonant transition in ^{57}Fe. The spectra were fitted within the transmission integral approach using the MOSGRAF–2009 software. Each sample was measured for 7 days.

2. The chemical composition and colour of samples after firing

The chemical analysis of the raw material from exploratory boreholes showed that the largest amounts of colouring oxides (Fe_2O_3 and TiO_2) are contained in the SI-1 sample (Table 1). Consequently, the pellets fired from that sample are characterised by the darkest colours (Fig. 1), which is reflected by low values of L* and a* colour parameters expressing lightness (brightness) and saturation of a red hue (when a > 0), respectively, while the value of b* (referring to yellow tint, when b > 0) is relatively high. The pellet SI-1c, which was fast-fired, differs from its counterpart fired in the standard cycle (SI-1j) by a greater intensity of the brown colour (lower L* and an over two-fold higher a*, with simultaneously lower b*).

In the case of sample SL-2 containing less colouring oxides than SI-1, higher values of a* and b* were obtained in the fast firing cycle than in the standard one, which was reflected in a warmer hue of the pastille. A similar result was observed for the pellets made of sample material PZ-3, which due to the relatively lowest content of Fe_2O_3 are characterized by the brightest tone among all the examined samples.

Fig. 1. Pellets SI-1j (left) and SI-1c (right) and the same peltets when cut

Fig. 1. Pastylki SI-1j (po lewej) i SI-1c (po prawej) oraz te same pastylki po przecięciu

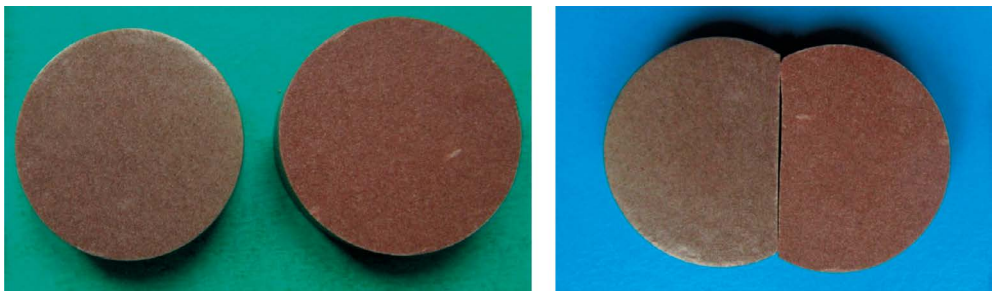

Fig. 2. Pellets SL-2j (left) and SL-2c (right) and the same peltets when cut

Fig. 2. Pastylki SL-2j (po lewej) i SL-2c (po prawej) oraz te same pastylki po przecięciu

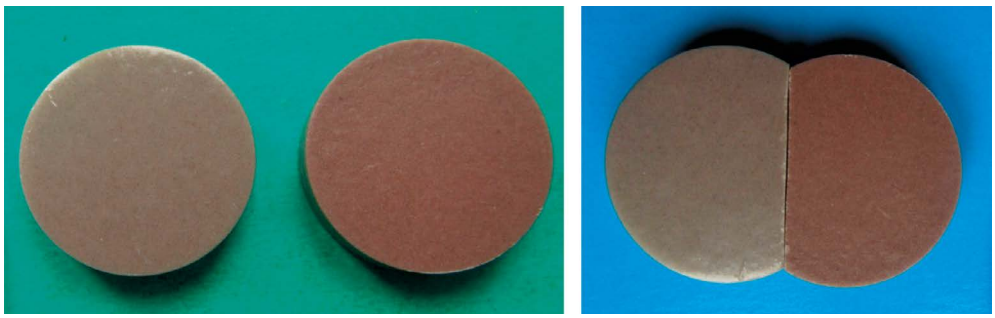

Fig. 3. Pellets PZ-3j (left) and PZ-3c (right) and the same peltets when cut

Fig. 3. Pastylki PZ-3j (po lewej) i PZ-3c (po prawej) oraz te same pastylki po przecięciu

Figures 1–3 show the pellets from the raw material of Strzeblów I (SI), Stary Łom (SL) and Pagórki Zachodnie (PZ) deposits after firing in different conditions (j – standard cycle > 2 h at a max. temperature of 1200°C, c – fast cycle lasting around 50 minutes at a max. temperature of 1260°C).

3. The results of X-ray powder diffraction studies

In the course of the thermal treatment of the samples, as the temperature rises, phase transitions as well as complete or partial melting of their mineral components are taking place. In order to assess the progress of these phenomena as well as to determine the mineral phases developed in the bodies obtained, X-ray powder diffraction of one pair of pellets PZ-3j and PZ-3c (fired in the standard and the fast cycle, respectively) was performed. The XRD pattern of the sample fired for more than 2 h (PZ-3j) showed that only residual quartz is present in the body (Fig. 4), as that mineral undergoes high-temperature phase transformations (from β to α variety at around 575°C, to α-tridymite – at 870°C and to α-cristobalite – at 1470°C), and melts completely at 1730°C (Fenner, fide: Wyszomirski and Galos 2007).

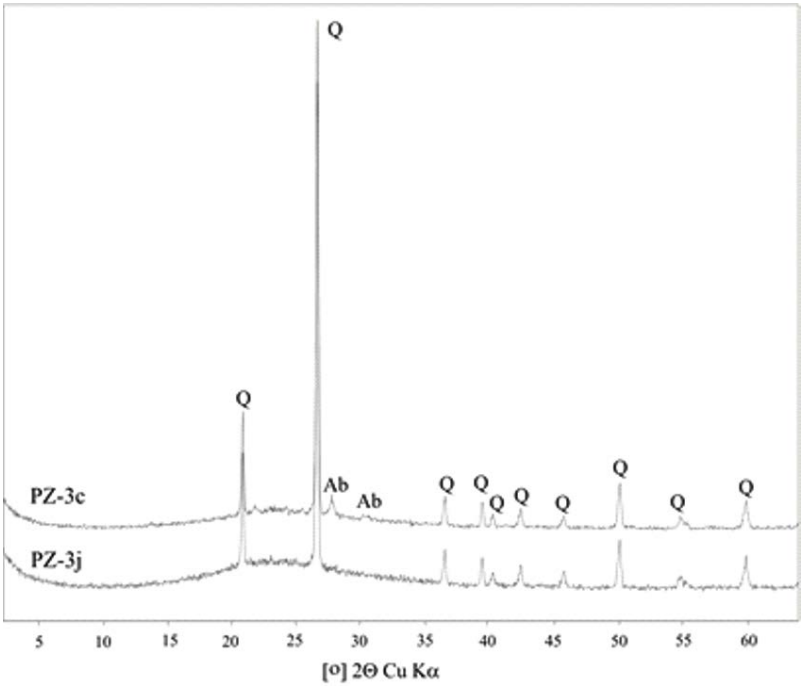

Fig. 4. XRD patterns of samples from the Pagorki Zachodnie deposit after firing in the standard (PZ-3j) and fast (PZ-3c) firing cycle

Fig. 4. Dyfraktogramy rentgenowskie próbek ze złoża Pagórki Zachodnie po wypaleniu w cyklu standardowym (PZ-3j) i szybkim (PZ-3c)

That sample contains a much more amorphous phase than the one fired in the fast cycle, as can be seen from the significantly higher background in angles ranging between 15 and 35° 2Θ CuKα. Apart from quartz some sodium feldspar, probably albite was identified on the XRD pattern of sample PZ-3c (Fig. 4). The remnants of crystalline Na-feldspar were observed at a temperature above the conventional temperature range of thermal stability of that mineral (pure albite melts congruently at 1118°C; Ehlers 1972) presumably because of the kinetics of reactions in a vitreous phase (Carty and Senapati 1998). The incomplete dissolution of sodium feldspar at 1260°C can be the result of a short soaking time (7 minutes) and fast, forced quenching of the examined sample.

4. The results of scanning microscopy (SEM-EDS) investigations

Scanning electron microscopy was performed on all the samples to investigate the evolution of the microstructure during firing in different conditions. It also provided information on ferruginous phases present in the fired bodies (Figs. 5–7).

The microstructure images of the fired bodies presented in Figures 5–7 show a comparison between pellets made of the same raw material but fired in different conditions: in the standard cycle (for more than 2 hours at a max. temperature of 1200°C) and the fast one (for around 50 minutes at a max. temperature of 1260°C). One of the most pronounced differences observed between them is more compact microstructure of the samples fired in the fast cycle than their counterparts. They are also characterized by a rough, uneven fracture with much less pores and bubbles visible on the surface, which indicates a better sintering of the bodies. The result of fast, forced cooling of the pastilles can also be areas closely resembling the glassy phase. On the other hand, the surface of the samples fired in the standard cycle (lasting more than 2 hours) and cooled to room temperature inside the furnace,

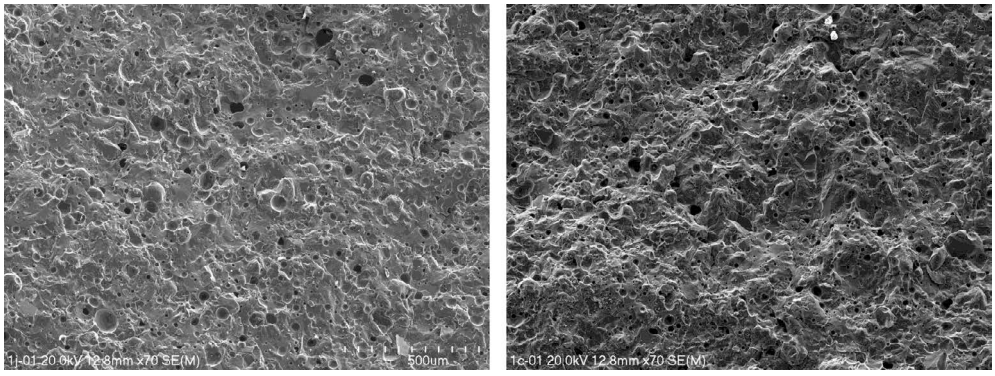

Fig. 5. Comparison of the microstructure of samples SI-1j (left) and SI-1c (right) fired under different conditions. SEM

Fig. 5. Porównanie mikrostruktury próbek SI-1j (po lewej) i SI-1c (po prawej) wypalonych w odmiennych warunkach. SEM

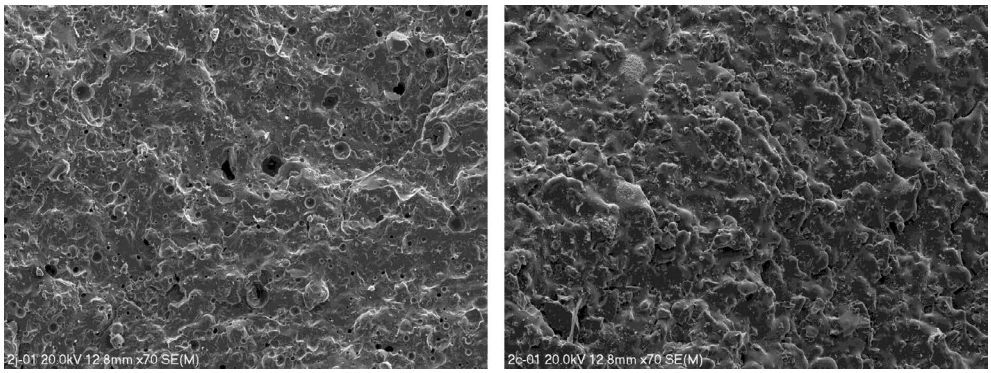

Fig. 6. Comparison of the microstructure of samples SL-2j (left) and SL-2c (right) fired under different conditions. SEM

Fig. 6. Porównanie mikrostruktury pastylek SL-2j (po lewej) i SL-2c (po prawej) wypalonych w odmiennych warunkach. SEM

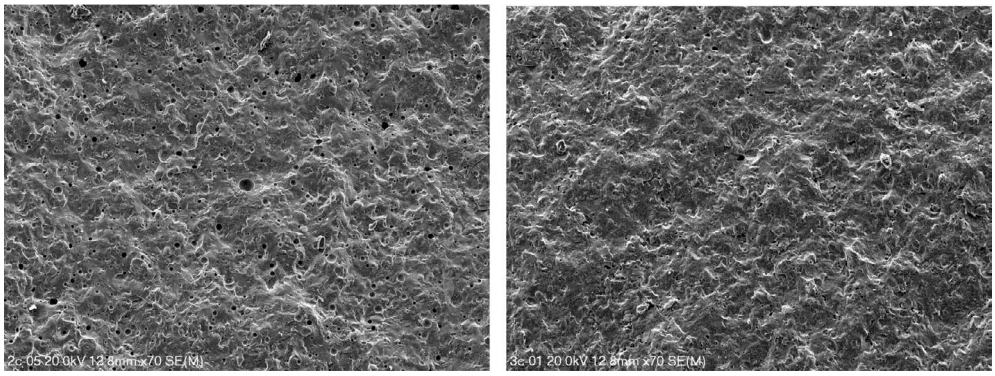

Fig. 7. Comparison of the microstructure of samples PZ-3j (left) and PZ-3c (right) fired under different conditions. SEM

Fig. 7. Porównanie mikrostruktury pastylek PZ-3j (po lewej) i PZ-3c (po prawej) wypalonych w odmiennych warunkach. SEM

is dotted by numerous, irregular pores of widely differing sizes, which probably resulted from the long-lasting gradual degassing of the body. The effect of this is increased porosity of the body.

The SEM-EDS analyses demonstrated that the basic component of the examined bodies is the melted aluminosilicate phase, resulting from the thermal decomposition of mainly feldspars and partly quartz (Figs. 8–9, 11, 14). In the course of the observations single quartz grains (Figs. 9, 11, 14) as well as other minerals with high melting temperatures, e.g. zircon (which decomposes incongruently at 1676°C giving off ZrO_2 and liquid rich in silica)

(Figs. 8–9, 11), were also found. Products of transformation of other mineral phases exposed to high temperature, such as: titanomagnetite or spinel Fe-Ti (Figs. 8–10 and 13-14), magnetite (Fig. 13), biotite (Figs. 8, 11–13), xenotime (Fig. 14), or sphalerite (Fig. 15) as well as probably chlorite (Fig. 13) and garnets (Fig. 12) were also observed relatively frequently (especially in the samples fired in the fast cycle).

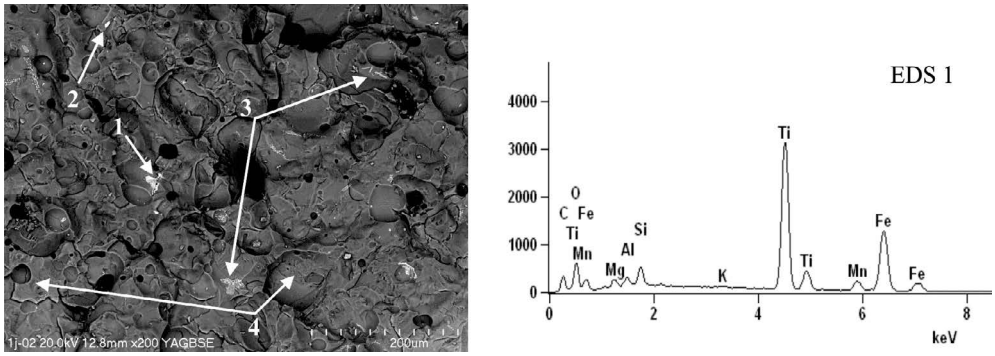

Fig. 8. SEM/BSE image of the sample from the Strzeblow I deposit:
1 – titanomagnetite (EDS 1), 2 – zircon, 3 – products of thermal decomposition of mica (biotite),
4 – aluminosilicate glassy matrix

Fig. 8. Próbka ze złoża Strzeblów I w obrazie SEM/BSE:
1 – tytanomagnetyt (EDS 1), 2 – cyrkon, 3 – produkty rozkładu mik (biotytu), 4 – stop glinokrzemianowy

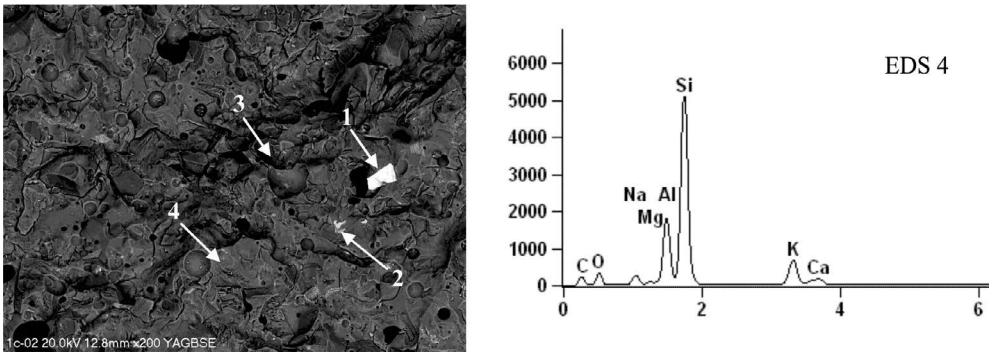

Fig. 9. SEM/BSE image of the sample from the Strzeblow I deposit:
1 – zircon, 2 – products of thermal decomposition of titanomagnetite, 3 – quartz,
4 – aluminosilicate glassy matrix (EDS 4)

Fig. 9. Próbka ze złoża Strzeblów I w obrazie SEM/BSE:
1 – cyrkon, 2 – produkty termicznego rozkładu tytanomagnetytu, 3 – kwarc,
4 – stop glinokrzemianowy (EDS 4)

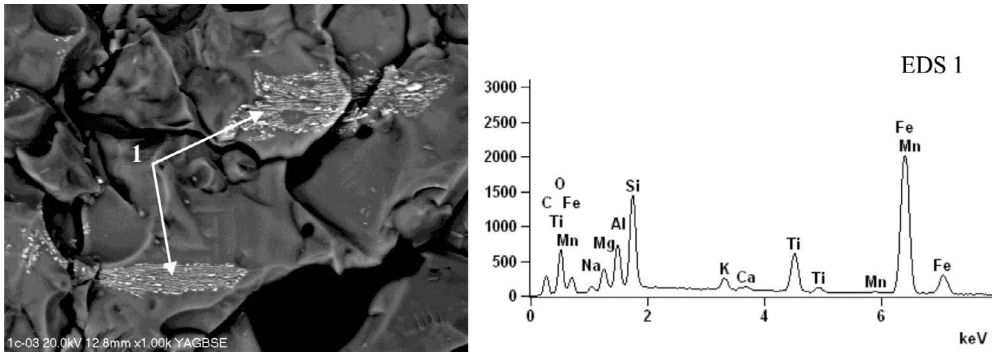

Fig. 10. Products of thermal decomposition of intergrowths of titanomagnetite and aluminosilicate phase (1, EDS 1) in the sample from the Strzeblow I deposit. SEM/BSE

Fig. 10. Produkty rozkładu termicznego przerostów tytanomagnetytu i fazy glinokrzemianowej (1, EDS 1) w próbce ze złoża Strzeblów I. SEM/BSE

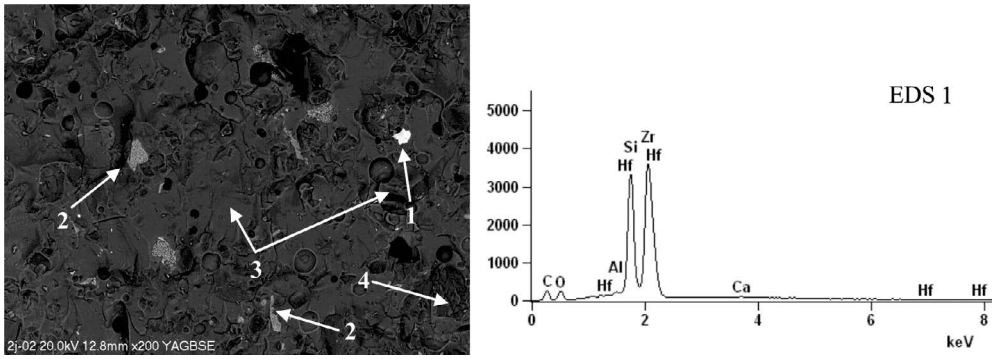

Fig. 11. SEM/BSE image of the sample from the Stary Lom deposit:
1 – zircon (EDS 1), 2 – products of decomposition of mica (biotite), 3 – aluminosilicate glassy matrix, 4 – quartz

Fig. 11. Próbka ze złoża Stary Łom w obrazie SEM/BSE:
1 – cyrkon (EDS 1), 2 – produkty rozkładu miki (biotytu), 3 – stop glinokrzemianowy, 4 – kwarc

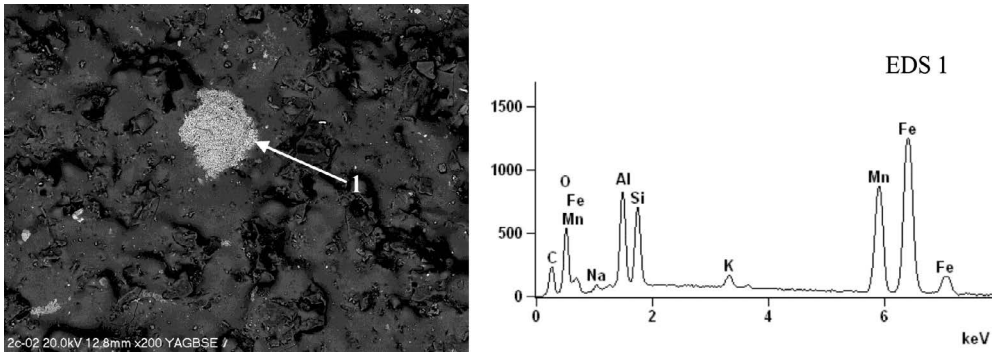

Fig. 12. Products of thermal decomposition of biotite (garnet?) (1, EDS 1) in the sample from the Stary Lom deposit. SEM/BSE

Fig. 12. Produkty rozpadu biotytu (granatu?) (1, EDS 1) w próbce ze złoża Stary Łom. SEM/BSE

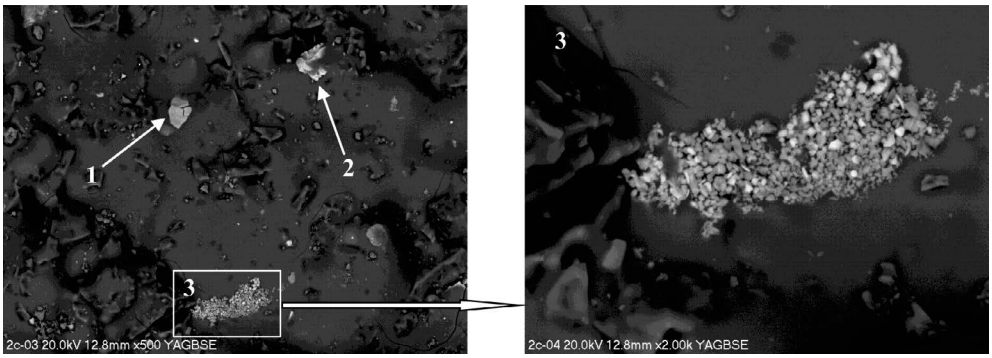

Fig. 13. SEM/BSE image of the sample from the Stary Lom deposit: 1 – titanomagnetite, 2 – magnetite, 3 – products of decomposition of biotite (chlorite?) – on the right in an enlarged view

Fig. 13. Próbka ze złoża Stary Łom w obrazie SEM/BSE: 1 – tytanomagnetyt, 2 – magnetyt, 3 – produkty rozkładu biotytu (chlorytu?) – po prawej stronie w powiększeniu

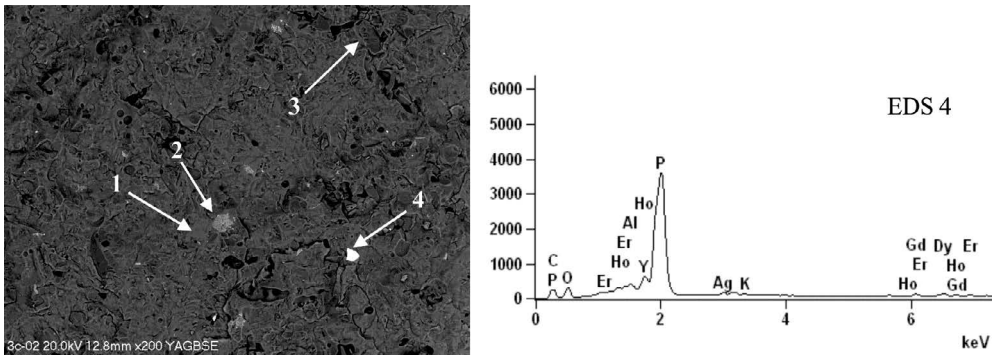

Fig. 14. SEM/BSE image of the sample from the Pagorki Zachodnie deposit: 1 – aluminosilicate glassy matrix, 2 – products of thermal decomposition of titanomagnetite, 3 – quartz, 4 – xenotime (EDS 4)

Fig. 14. Próbka ze złoża Pagórki Zachodnie w obrazie SEM/BSE: 1 – stop glinokrzemianowy, 2 – produkty rozkładu termicznego tytanomagnetytu, 3 – kwarc, 4 – ksenotym (EDS 4)

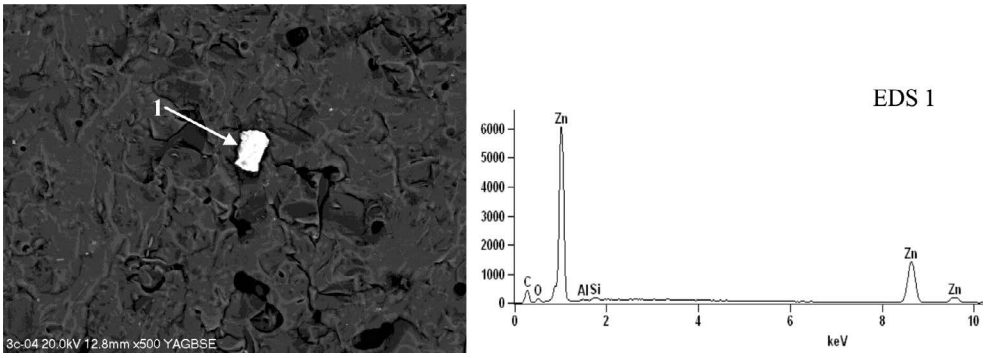

Fig. 15. Product of thermal decomposition of sphalerite (1) in the sample from the Pagorki Zachodnie deposit. SEM/BSE-EDS

Fig. 15. Produkt rozkładu termicznego sfalerytu (1) w próbce ze złoża Pagórki Zachodnie. SEM/BSE-EDS

5. The results of the Mössbauer spectroscopy studies

The results of the Mössbauer measurements were of basic significance for the qualitative and quantitative assessment of the oxidation state of iron and identification of ferruginous phases in the fired bodies (Table 2). The research was conducted on one pair of pellets made of the raw material SI-1, characterized by the relatively highest content of Fe_2O_3 (1.7%). The products of thermal treatment in different conditions (firing in the standard and the fast cycle, respectively) were the bodies that significantly differ in colour (Fig. 1).

From the point of view of Mössbauer spectroscopy, both samples are very similar to each other (Table 2). The spectra recorded at room temperature do not show any clear lines from Fe^{2+}, which can indicate that the iron was wholly oxidised in the course of firing. The contribution of paramagnetic component of Fe^{3+} in both samples is similar (around 30%). The spectra also include doublets corresponding to iron ions of an averaged oxidation state 2.5+ ($Fe^{2+/3+}$), the hyperfine parameters of which, i.e. QS (ca. 2.3) is typical for Fe^{2+}, while IS (around 0.5 mm/s) is characteristic for Fe^{3+} in octahedral sites (Dyar 1985; Mysen 2006). The percentage of this form of iron is relatively low, although the light-coloured pellet SI-1j fired in the standard cycle for more than 2 hours contains $Fe^{2.5+}$ twice as much as

Table 2. Hyperfine parameters of Mössbauer spectra of SI-1j and SI-1c samples

Tabela 2. Parametry mössbauerowskie widm próbek SI-1j i SI-1c

Sample	Form of iron	W [%]	IS [mm/s]	QS [mm/s]	B [T]	Γ [mm/s]
SI-1c	Fe_2O_3 well crystallised	8±2	0.36±0.01	–0.23±0.01	50.4±0.1	0.19±0.01
	Fe_2O_3 poorly crystallised	22±10	0.37±0.01	–0.21±0.01	48.3±0.1	0.61±0.01
	Fe-O (nanocrystalline phase ?)	35±11	0.1±0.2	–	28±1	3±1
	Fe^{3+}	30±9	0.34±0.01	0.82±0.01	–	0.79±0.01
	$Fe^{2+/3+}$	5±2	0.49±0.01	2.26±0.01	–	0.45±0.01
SI-1j	Fe_2O_3 well crystallised	11±2	0.36±0.01	–0.23±0.01	50.6±0.1	0.21±0.01
	Fe_2O_3 poorly crystallised	19±7	0.37±0.01	–0.22±0.01	48.6±0.1	0.49±0.01
	Fe-O (nanocrystalline phase ?)	29±7	0.4±0.2	–	30±1	3±1
	Fe^{3+}	31±8	0.32±0.01	0.89±0.01	–	0.73±0.01
	$Fe^{2+/3+}$	10±3	0.52±0.01	2.29±0.01	–	0.72±0.01

W – relative contribution of the given iron form (sub-spectrum), IS – isomer (total) shift versus α-Fe, QS – quadrupole splitting, B – magnetic hyperfine field, Γ – absorber line-width

for another one – SI-1c of a darker hue (10 and 5%, respectively). However, that difference cannot be a reason for their colour dissimilarity after firing. The spectra of both samples consist of paramagnetic doublets referring to the above-mentioned ions (Fig. 16 – green line for Fe^{3+} and orange one – for $Fe^{2.5+}$).

The hyperfine parameters of Fe^{3+} ions, i.e. isomer shift and quadrupole splitting, suggest that they can be dispersed in iron-bearing paramagnetic aluminosilicate glass (Table 2, Szumiata et al. 2014, see: Stevens et al. 2005), while the line of iron of mixed valence, show-

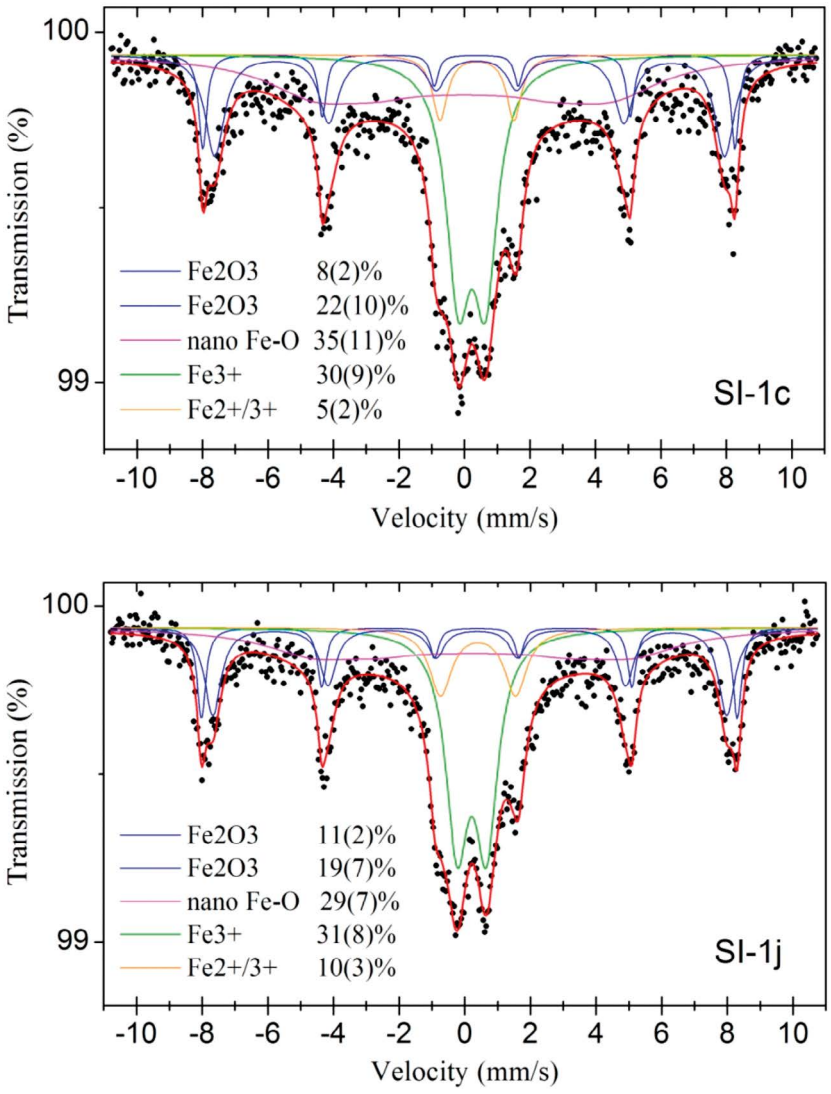

Fig. 16. Room temperature Mössbauer spectra of SI-c and SI-1j samples

Fig. 16. Eksperymentalne widma mössbauerowskie próbek SI-1c i SI-1j (pomiar w temperaturze pokojowej)

ing paramagnetic behaviour at room temperature, is supposed to be the result of the substitution of Fe^{3+} by Ti^{4+} (and the consequent reduction of Fe^{3+} to Fe^{2+} to maintain a charge balance) as stated in the structure of titanomagnetite (Sorescu et al. 2012). Eventually, due to possible coexistence of both Fe^{3+} and Fe^{2+} in the same (octahedral) structural site, an average oxidation state of 2.5+ can be assumed. This hypothesis was investigated by Sorescu et al. (2012), studying the effect of progressive substitution of iron by titanium in a titanomagnetite solid solution in the pseudo-binary system $Fe^{2+}_2TiO_4$–$Fe^{2+}Fe^{3+}_2O_4$, synthesised at high temperatures. They observed a gradual decline of the strength of the hyperfine magnetic field with an increasing content of Fe_2TiO_4 and the appearance of a broad quadrupole doublet instead of magnetic sextet. This reasoning is in good agreement with the results of scanning microscopy observations presented in the article, that revealed the concentrations of phases reach in Fe and Ti, described as titanomagnetite or as products of its thermal decomposition (Figs. 8–10 and 14).

The recorded Mössbauer spectra of both samples also contain two superimposed magnetic hyperfine sextets that can be assigned to Fe_2O_3 (blue lines) occurring in two varieties – well and poorly crystallised (of distorted structure, being possibly a result of substitution of Fe^{3+} by Al^{3+}, see: Bowen and De Grave 1995). This is evidenced by the difference between lines widths, especially in the case of the sample SI-1c (Γ = 0.19 and 0.61 mm, respectively). The combined contribution in the spectra of Fe_2O_3 approached 30% (in relation to all phases containing iron ΣFe). The hyperfine parameters of these lines suggest that they can refer to hematite in various stages of either phase transformation (Table 2, see: Stevens et al. 2005).

The third important component of the examined samples, the relative content of which equals 29% (in the light-coloured pellet) and 35% (in the dark-coloured one), is a phase of iron oxide (Fe-O), manifesting itself by the wide diffused line (pink). Its ferruginous nature is suggested by the value of the isomer shift (IS), as well as by the presence of hyperfine magnetic field (B) (Table 2). Due to the very low signal, the measurement of QS is impossible to be carried out. It can be assumed that this phase arises at an elevated temperature and remains almost amorphous or poorly crystalline after cooling (therefore, it can be described as a 'nanocrystalline'). This interpretation can be supported by the Mössbauer studies of iron-bearing silicate glasses composed of SiO_2–Fe_2O_3–Na_2O, which demonstrated that very fine particle size or amorphous nature may also hamper the detection of ferruginous components present in the 'glassy' phase (Burkhard 2000). The difficulties in quadrupole splitting (QS) measurement can also be attributed to the substitution of iron by other elements present in the vitreous phase (e.g. Ti or Mn, released in the course of thermal decomposition of their mineral carriers). Furthermore, the registered signal can belong to more than one coexisting iron phases and/or to newly formed species in the melt. Mössbauer parameters of the spectra of that problematic component suggest that it can be related to one of the ferruginous minerals observed in the scanning microscope – magnetite, titanomagnetite or their remnants, whether to products of thermal decomposition of iron-rich biotiote, garnet or chlorite (Table 2, see: Stevens et al. 2005).

The isomer shift of ferric iron Fe^{3+} in both samples (IS = 0.32–0.34) can refer to tetrahedral site in the crystal lattice (Steffen et al. 1984; Spiering and Seifert 1985; Mysen 2006). That is confirmed by the results of the investigations carried out on various glasses obtained by melting their constituents under an oxidative atmosphere (e.g. Burkhard 2000; Zawada 2009), i.e. analogous to the conditions of experiments presented in this article.

6. Discussion

The components of the ceramic bodies undergo thermal transformations and complex phase transitions in the course of firing. Their evolution is greatly influenced by the presence of transition elements, especially iron, their oxidation state and structural position. The studies dealing with this issue demonstrated that the majority of iron-bearing phases when exposed to a high temperature was spontaneously converted into hematite crystals surrounded by an aluminosilicate melt, while only a small portion of them participated in structural transformations and thickening of the vitreous phase (Andji et al. 2009). This was also confirmed that under heat and contact with alkali melt both the coordination and valence state of iron can change from Fe^{2+} in octahedral site to Fe^{3+} in the tetrahedral one. It can promote phase transitions with the formation of hematite (Fe_2O_3) in an oxygen environment (Lassinantti et al. 2011). These findings are consistent with the results of research carried out within a frame of this work by Mössbauer spectroscopy and scanning microscopy SEM-EDS. Previous studies of raw feldspar-quartz samples by Mössbauer method showed that the raw material characterized by prevalence of Fe^{2+} over Fe^{3+} were much darker in colour after firing than the samples, in which ferric ions dominated (Lewicka 2016a, 2016b). Current investigations revealed that the majority of iron ions in the examined fired bodies is in trivalent state of oxidation and probably occupies the tetrahedral sites. According to the literature such coordination influences the colour of the body after firing much more than location of Fe^{3+} in the octahedral one (vide Sikora 1974; Dziubak 2012). Also, the presence of other transition elements is not without merit, providing the modification of colour caused by iron (Burns and Dyar 1981; Dyar 1985). This refers especially to titanium and manganese that were detected in the samples in course of SEM-EDS studies. These elements have strong colouring properties and/or ability to modify colour, as it has already been discussed in previous papers published by the author (Lewicka 2015, 2016a, 2016b). Concentrations of small crystallites of ferruginous phases rich in Mn observed under scanning microscope (Fig. 12) can be a result of common substitution of Mn and Fe of the same valence, i.e. Mn^{2+} and Fe^{2+}, in their mineral carriers (garnets, micas, chlorites), being components of the feldspar-quartz raw materials utilised for the pellets making. In course of annealing, high temperature and oxygen atmosphere favour the formation of bonds between manganese and iron, that – at around 1150°C – can result in the development of manganese oxide (III) and hematite (Konratowska 2010; Ding et al. 1997).

www.czasopisma.pan.pl PAN POLSKA AKADEMIA NAUK www.journals.pan.pl

Conclusions

The Mössbauer spectroscopy studies were of fundamental significance for the assessment of forms and the oxidation state of iron occurring in the examined fired bodies. They revealed that Fe^{2+} ions were wholly oxidised to Fe^{3+}, which changed the coordination site to the tetrahedral one. The presence of other transition elements, especially titanium and manganese, probably also influenced the colour of the bodies obtained. It is assumed that concentrations of Fe,Mn-rich crystallites observed under scanning microscope can be a result of the formation of bonds between manganese and iron and consequent development of manganese oxide and hematite at a high temperature and under oxidative conditions. Mössbauer studies demonstrated the presence of three basic components constituting around 30% (each) of the spectra of both samples, i.e. Fe_2O_3 (presumably hematite), Fe^{3+} ions (dispersed in aluminosilicate glassy phase), and nanocrystalline ('amorphous') oxide phase of iron Fe-O. Some relatively small amounts (5 and 10%) of mixed valence iron ions ($Fe^{2+/3+}$) that are not expected to cause the colour difference between samples after firing were also found. They are suspected to be incorporated into the structure of spinel described as a titanomagnetite in the course of SEM-EDS studies.

The interpretation of colour variability of the examined samples after firing is a difficult and complex issue. The major reason for this seems to be different conditions of thermal treatment of the samples, i.e. various temperatures, soaking time, and quenching (cooling rate), that resulted in difference in the sintering degree and possibly – in the advancement of phase transitions in non-equillibrium systems. Therefore, it can be assumed that in the course of fast firing (at max. 1260°C) and rapid quenching of the sample SI-1c (of darker hue), iron and/or other colouring elements were incompletely incorporated into the structure of the developing phases (to be hidden), and – as a consequence – remained in the glassy matrix in dispersed form or as a 'nanocrystalline' (?) Fe-O phase. This is supported by the fact that relative contribution of the latter in the Mössbauer spectrum of the darker sample is larger than in its counterpart fired in the standard cycle (at max. 1200°C) and slowly quenched that probably resulted in a lighter colour of the obtained ceramic body.

The above-mentioned observations and results of the research lead to the conclusion that the main reason for colour variation in the examined bodies as well as their different microstructure and advancement of phase transitions in course of firing are different conditions of thermal treatment. These probably also influenced the forms in which iron and other colouring elements occur in the samples.

REFERENCES

Andji et al. 2009 – Andji, J.Y.Y., Abba Toure, A., Kra, G., Jumas, J.C., Yvon, J. and Blanchart, P. 2009. Iron role on mechanical properties of ceramics with clays from Ivory Coast. *Ceramics International* 35, pp. 571–577.

Bowen, L.H. and De Grave, E. 1995. Mössbauer spectra in external field of highly substituted aluminous hematites. *Journal of Magnetism and Magnetic Minerals* 139, pp. 6–120.

www.czasopisma.pan.pl PAN POLSKA AKADEMIA NAUK www.journals.pan.pl

Burkhard, D.J.M. 2000. Iron-bearing silicate glasses at ambient conditions. *Journal of Non-Crystalline Solids*, 275, pp. 175–188.

Burns, R.G. and Dyar, M.D. 1981. Coordination chemistry of iron in natural and synthetic glasses. Geological Society of America Abstracts with Programs, 420.

Carty, W.M., and Senapati, U. 1998. Porcelain: raw materials, processing, phase evolution and mechanical behaviour. *Journal of American Ceramic Society* 81, pp. 3–20.

Ding et al. 1997 – Ding, J., McCormick, P.G. and Street, R. 1997. Formation of spinel Mn-ferrite during mechanical alloying. *Journal of Magnetism and Magnetic Minerals* 171, pp. 309–314.

Dyar, M.D. 1985. A review of Mössbauer data on inorganic glasses: the effects of composition on iron valence and coordination. *American Mineralogist* 70, pp. 304–316.

Dziubak, C. 2012. Fizykochemiczne podstawy syntezy ceramicznych pigmentów cyrkonowych. Kraków: *Ceramika/Ceramics* 112, pp. 179 (*in Polish*).

Ehlers, E.G. 1972. *The interpretation of geological phase diagrams*. San Francisco: W.H. Freeman and Company.

Górnicki et al. 2007 – Górnicki, R., Błachowski, A. and Ruebenbauer, K. 2007. Mössbauer Spectrometer MsAa-3. *Nukleonika* 52 (suppl.1), S7.

Konratowska, A., 2010. Otrzymywanie, właściwości i zastosowanie wybranych tlenków i hydroksytlenków żelaza. Praca doktorska. Zachodniopomorski Uniwersytet Technologiczny. Wydział Technologii i Inżynierii Chemicznej i Procesowej (*in Polish*).

Lassinantti et al. 2011 – Lassinantti, G.M., Ramagnoli, M. and Gualtieri, A.F. 2011. Influence of body composition on the technological properties and mineralogy of stoneware: A DOE and mineralogical-microstructural study. *Journal of the European Ceramic Society* 31, pp. 673–685.

Lewicka, E. 2013. Barwa po wypaleniu a skład mineralny kopalin skaleniowych z rejonu Sobótki. *Gospodarka Surowcami Mineralnymi – Mineral Resources Management* vol. 29, issue 1, pp. 35–51 (*in Polish*).

Lewicka, E. 2015. Badanie wpływu domieszek żelaza na parametry barwy kopalin skaleniowo-kwarcowych po wypaleniu. *Gospodarka Surowcami Mineralnymi – Mineral Resources Management* vol. 31, issue 1, pp. 81–94 (*in Polish*).

Lewicka, E. 2016a. The studies of granitoids from the Sobótka region in light of theories of the origin of colour in minerals. *Gospodarka Surowcami Mineralnymi – Mineral Resources Management* vol. 32, issue 1, pp. 55–69.

Lewicka, E., 2016b. Origin of colour after firing of feldspar-quartz raw material from the Sobotka region (Lower Silesia, SW Poland). *E3S Web of Conferences* 8, 01022 (2016), DOI: 10.1051/e3sconf/20160801022, pp. 1–8.

Lewicka, E. and Franus, W. 2014. Badania przyczyn niejednorodności surowca skaleniowo-kwarcowego po wypaleniu. *Gospodarka Surowcami Mineralnymi – Mineral Resources Management* vol. 30, issue 1, pp. 69–83 (*in Polish*).

Mysen, B.O. 2006. The structural behaviour of ferric and ferrous iron in aluminosilicate glass near meta-aluminosilicate joins. *Geochimica et Cosmochimica Acta* 70, pp. 2337–2353.

Sikora, W. 1974. Żelazo w kaolinach pierwotnych Dolnego Śląska. *Prace Mineralogiczne* 39. Warszawa: Wydawnictwa Geologiczne, p. 76 (*in Polish*).

Sorescu et al. 2012 – Sorescu, M., Xu, T., Wise, A., Diaz-Michelen, M. and McHenry, M.E. 2012. Studies on structural, magnetic and thermal properties of $x Fe_2TiO_4$-$(1-x)Fe_3O_4$ ($0 \leq x \leq 1$) pseudo-binary system. *Journal of Magnetism and Magnetic Materials* 324. Elsevier, pp. 1453–1462.

Spiering, B. and Seifert, F. A. 1985. Iron in silicate glasses of granitic composition: a Mössbauer spectroscopic study. *Contributions to Mineralogy and Petrology*. Springer-Verlag, pp. 63–73.

Steffen et al. 1984 – Steffen, G., Seifert, F.A. and Amthauer, G. 1984. Ferric iron in sapphirine: A Mössbauer spectroscopic study. *American Mineralogist* 69, pp. 339–349.

Stevens et al. 2005 – Stevens, J.G., Khansanov, A.M., Miller, J.W., Pollak, H. and Li, Z. 2005. Mössbauer Mineral Handbook. Mössbauer Effect Data Center. Asheville (USA).

Szumiata et al. 2014 – Szumiata, T., Brzózka, K., Górka, B., Gawroński, M., Gzik-Szumiata, M., Świetlik, R. and Trojanowska, M. Iron speciation in coal-fly ashes – chemical and Mössbauer analysis. *Hyperfine Interactions* 226, pp. 483–487.

Wyszomirski, P. and Galos, K. 2007. Surowce mineralne i chemiczne przemysłu ceramicznego. Kraków: Uczelniane Wydawnictwa Naukowo-Dydaktyczne AGH, pp. 283 (*in Polish*).

www.czasopisma.pan.pl PAN POLSKA AKADEMIA NAUK www.journals.pan.pl

Zawada, A. 2009. Lokalizacja jonów żelaza w strukturze szkieł krzemianowych. Szkło i Ceramika 60 (5). Warszawa: Instytut Ceramiki i Materiałów Budowlanych, pp. 25–32 (*in Polish*).

PRZEMIANY FAZOWE NOŚNIKÓW ŻELAZA PODCZAS OBRÓBKI TERMICZNEJ KOPALIN SKALENIOWO-KWARCOWYCH Z REJONU SOBÓTKI (DOLNY ŚLĄSK)

Słowa kluczowe

fazy żelaziste, przemiany fazowe, spektroskopia mössbauerowska, kopalina skaleniowo-kwarcowa, barwa po wypaleniu

Streszczenie

Opracowanie przedstawia wyniki badań kopaliny skaleniowo-kwarcowej pochodzącej ze złóż leukogranitów z rejonu Sobótki. Jest to kolejny etap prowadzonych przez autorkę badań nad wpływem składu chemicznego i mineralnego tych utworów na barwę uzyskanych z nich tworzyw ceramicznych. Obejmował on wypalanie par próbek o analogicznym składzie chemicznym w odmiennych warunkach: w cyklu standardowym, trwającym ponad 2 godziny (w maksymalnej temperaturze 1200°C), oraz szybkim, około 50-minutowym (w maks. 1260°C). Uzyskane tworzywa zostały poddane analizie rentgenowskiej, a także badaniom metodą mikroskopii skaningowej SEM-EDS i spektroskopii mössbauerowskiej w temperaturze pokojowej. Analiza rentgenowska ujawniła obecność kwarcu w obu próbkach, a w przypadku pastylki wypalonej w krótkim cyklu – również reliktów skalenia sodowego. Badania skaningowe potwierdziły, że podstawowym składnikiem badanych tworzyw jest stop glinokrzemianowy, który powstał w wyniku termicznego rozkładu głównie skaleni i częściowo kwarcu. W toku obserwacji stwierdzono obecność pojedynczych ziaren kwarcu oraz innych minerałów cechujących się wysoką temperaturą topienia, takich jak cyrkon. Stosunkowo często obserwowano także produkty przeobrażenia pod wpływem wysokiej temperatury innych faz mineralnych, takich jak: tytanomagnetyt (spinel Fe-Ti), biotyt, ksenotym, sfaleryt oraz przypuszczalnie chloryty i granaty. Badania mössbauerowskie wykazały obecność w tworzywie trzech równorzędnych składowych o względnych zawartościach rzędu 30% każda: Fe_2O_3 (przypuszczalnie hematyt), kationów Fe^{3+} (rozproszonych w stopie glinokrzemianowym) oraz słabo krystalicznej względnie amorficznej fazy tlenkowej żelaza (Fe-O). Stwierdzono również występowanie podrzędnej ilości kationów żelaza o mieszanej walencyjności ($Fe^{2+/3+}$), których względny udział w obu próbkach jest niewielki (10 i 5%) i – jak się przypuszcza – nie może przesądzać o zróżnicowaniu ich zabarwienia. Odpowiadający im dublet paramagnetyczny ma przypuszczalnie związek z obecnością tytanomagnetytu lub produktów jego rozkładu termicznego. Powyższe obserwacje i uzyskane wyniki badań skłaniają do stwierdzenia, że główną przyczyną zróżnicowania barwy próbek są odmienne warunki ich obróbki termicznej, w wyniku czego uzyskano tworzywa różniące się stopniem spieczenia oraz zaawansowania przemian fazowych , co zapewne rzutowało na formę związania żelaza i innych pierwiastków barwiących.

www.czasopisma.pan.pl PAN POLSKA AKADEMIA NAUK www.journals.pan.pl

PHASE TRANSITIONS OF FERRUGINOUS MINERALS IN THE COURSE OF THERMAL PROCESSING OF FELDSPAR-QUARTZ RAW MATERIALS FROM THE SOBÓTKA REGION (LOWER SILESIA)

Keywords

ferruginous phases, phase transitions, Mössbauer spectroscopy,
feldspar-quartz raw material, colour after firing

Abstract

This paper presents the results of analyses of feldspar-quartz raw materials from deposits of leucogranites located in the Sobótka region. This is a successive stage of research carried out by the author on reasons for colour variation of ceramic materials obtained from them. This step encompassed the firing of sample pairs of analogous chemical composition in different conditions: in a standard cycle lasting more than 2 hours (at a maximum temperature of 1200°C), and a fast one – lasting around 50 minutes (at a max. temperature of 1260°C). The obtained ceramic bodies were analysed using the XRD method, scanning microscopy SEM-EDS and ^{57}Fe Mössbauer spectroscopy at room temperature. The XRD investigations revealed the presence of quartz in both samples, while remnants of sodium feldspar were observed in the one fired in the fast cycle. The scanning microscopy confirmed that the principal component of the examined bodies is the aluminosilicate melt, resulting from the thermal decomposition of mainly feldspars and quartz. Single quartz grains and other minerals of high melting temperatures, i.e. zirconium, were also observed in the course of microscopic examinations. Products of other mineral phases' transformations at high temperature, such as: titanomagnetite (spinel Fe-Ti), magnetite, biotite, xenotime, sphalerite as well as probably chlorites and garnets, were also relatively frequent. Mössbauer studies demonstrated the presence of three basic components constituting 30% (each) of the spectra, i.e. Fe_2O_3 (presumably hematite), Fe^{3+} ions (dispersed in aluminosilicate glassy phase), and nanocrystalline or amorphous oxide phase of iron (Fe-O). Some relatively small amounts (5 and 10%) of mixed valence iron cations ($Fe^{2+/3+}$) that are not expected to influence the colour difference between samples after firing were also found. A paramagnetic doublet referring to them can be attributed to a titanomagnetite spinel or products of its thermal decomposition. The above-mentioned observations and examinations lead to the finding that the main reason for colour variation in the examined bodies as well as their different microstructure and advancement of phase transitions in the course of firing are different conditions of thermal treatment. These probably also influenced the forms in which iron and other colouring elements occur in the samples studied.